THE JOURNAL OF PHYSICAL CHEMISTRY B LETTERS

2006, *110,* 17296−17301
Published on Web 08/17/2006

Surface-Enhanced Raman Spectroscopic Evidence of Methanol Oxidation on Ruthenium Electrodes

Hongzhou Yang, Yuqing Yang, and Shouzhong Zou*

Department of Chemistry and Biochemistry, Miami University, Oxford, Ohio 45056

Received: June 13, 2006; In Final Form: July 19, 2006

Electrooxidation of methanol on Ru surfaces was investigated using in situ surface-enhanced Raman spectroscopy. Although the cyclic voltammogram did not show a significant methanol oxidation current on Ru, a Raman band at ~1970−1992 cm^{-1} was observed from 0.4 to 0.8 V in 0.1 M $HClO_4$ + 1 M methanol. By comparing with the C−O stretching band (ν_{CO}) of carbon monoxide (CO) adsorbed on RuO_2(110) in the ultrahigh vacuum and on oxidized Ru electrodes, the observed spectral feature is assigned to ν_{CO} of adsorbed CO (CO_{ads}) on RuO_2. The formation of CO_{ads} suggests that methanol oxidation does occur on Ru at room temperature, which is in contrast to the perception that Ru is not active for the reaction. The lack of significant methanol oxidation current is attributed to the competing rapid surface oxidation, which forms inactive surface oxides and therefore inhibits the methanol oxidation.

Introduction

Ruthenium modified Pt, either in the form of a Ru decorated Pt surface or a Pt−Ru alloy, is so far the best anode catalyst for the direct methanol fuel cell (DMFC).[1−3] The high activity of Pt−Ru for the methanol oxidation is generally explained in terms of the so-called "bifunctional mechanism".[4] In this mechanism, methanol dissociation occurs on Pt sites to form carbon monoxide (CO), which is a surface poison that blocks further methanol oxidation, and the Ru sites provide oxygen containing species to oxidize CO at a lower potential than on pure Pt. Another mechanism for the Ru enhancement of methanol oxidation is the so-called ligand effect or electronic effect.[5−8] The presence of Ru decreases the CO adsorption energy on Pt, therefore further facilitating its oxidation. In both mechanisms, the role of Ru is to facilitate the CO oxidation and methanol oxidation on Ru sites is generally not considered.

Compared to the extensive work on Pt−Ru surfaces,[1−3] the study of CO and methanol oxidation on Ru is relatively sparse. Leung and Weaver studied the adsorption and electrooxidation of CO on Ru thin films with surface-enhanced Raman spectroscopy.[9] Iwasita and co-workers compared the CO adsorption and oxidation on Ru, Pt, and PtRu using in situ Fourier transform infrared (FTIR) spectroscopy and found that among the three surfaces Ru is the best catalyst for solution-phase CO oxidation.[10] Lin et al. studied CO adsorption and oxidation on Ru(0001) using in situ FTIR as well as ex situ electron diffraction and Auger spectroscopy.[11] Different from the polycrystalline Ru where only atop CO was observed, both atop and threefold bound CO were reported.[11,12] In agreement with these surface IR results, a c(2 × 2)-2CO adlayer on Ru(0001) with a CO coverage of 0.5 was revealed by in situ scanning tunneling microscopy (STM).[13] Methanol oxidation on Ru is considered insignificant at room temperature, as no significant methanol oxidation current was observed on polycrystalline Ru in the acidic media.[14−16] However, at elevated temperatures (>50 °C), significant methanol oxidation was observed and the activity increases with increasing temperature.[14−17] This temperature-dependent activity was accounted for by the desorption of inhibiting surface oxides as well as the activation of water at higher temperatures.[16,17] On the basis of in situ FTIR studies on Ru(0001), it is concluded that methanol oxidation does not occur below 0.9 V (vs Ag/AgCl) in the acidic solution at both 20 and 55 °C.[18−20] Interestingly, in alkaline media, atop bound CO_{ads} on the same surface was observed at −0.8 to +0.4 V at both temperatures, suggesting that the surface is active for methanol oxidation.[20]

Surface-enhanced Raman spectroscopy (SERS) with its high surface sensitivity and its ability to detect vibration modes as low as 100 cm^{-1} can provide information about methanol oxidation on Ru or Ru modified Pt that is not readily available with in situ FTIR.[21,22] Surprisingly, there is only one prior SERS study on methanol oxidation on Ru modified Pt by Tian's group.[23]

In this Letter, we report a surface-enhanced Raman study of methanol oxidation on Ru thin films electrodeposited on Au surfaces. Although the voltammograms obtained on Ru in solutions with and without methanol are essentially identical up to 0.8 V, a C−O stretching band from CO_{ads} on Ru oxide (RuO_2) was detected in the presence of methanol at potentials where Ru is significantly oxidized. The results for the first time reveal that methanol oxidation in acidic media does occur at room temperature on Ru surfaces at the potentials where the methanol oxidation peak current is typically observed on Pt−Ru catalysts. The insignificant methanol oxidation current on Ru is attributed to the facile surface oxidation and the inactive

* To whom correspondence should be addressed. Phone: 513-529 8084. Fax: 513-529 5715. E-mail: zous@muohio.edu.

10.1021/jp063694s CCC: $33.50

nature of Ru oxide toward the reaction. The study sheds light on the mechanism of methanol oxidation on the Ru surface and may provide useful information for designing more efficient anode catalysts for DMFCs.

Experimental Section

To obtain the surface-enhanced Raman effect, a Au electrode (2 mm in diameter, CH Instruments, Austin, TX) was polished successively with 1.0 and 0.3 μm Al_2O_3 powder on a polishing cloth (Buehler, Lake Bluff, IL) and roughened by electrochemical oxidation−reduction cycles in 0.1 M KCl, as described by Gao et al.[24] Ruthenium was deposited onto the roughened Au by constant potential deposition at −0.05 V in deaerated 1 mM $RuCl_3$ + 0.1 M $HClO_4$ aqueous solution.[9] The deposition time is typically 60 s, yielding Ru films with a nominal thickness of three to five monolayers, as estimated from the faradaic charge involved in the deposition and assuming 100% current efficiency. In situ scanning tunneling microscopic images obtained on Au(111) showed that multilayer Ru films are formed under the deposition conditions used here.[25]

Cyclic voltammograms were recorded with an electrochemical analyzer (CHI630A, CH Instruments, Austin, TX). SERS measurements were conducted in a two-compartment, three-electrode glass cell with an optically flat glass disk as the window at the bottom. A Pt wire was used as the counter electrode, and the reference electrode is a Ag/AgCl electrode with saturated KCl (CH Instruments). The electrode potential was controlled by a voltammograph (CV27, BAS, West Lafayette, IN). Raman spectra were collected with a portable micro-Raman probe system, as described elsewhere.[26,27] Briefly, a laser excitation at 785 nm from a diode laser was focused to a 100 μm spot on the sample with a long working distance 20× microscope objective (NA 0.42). The Raman scattering light was collected with the same objective in a backscattering fashion and sent to a monochromator. The laser power on the sample is typically 20 mW. The Raman shift axis was calibrated with a neon light. The typical spectrum acquisition time was 30 s unless otherwise noted. A 300 groove/mm grating was used, which yields a spectral range of 280−3200 cm^{-1}. However, only the interesting frequency regions (oxide vibration and C−O stretching) are shown. The spectra were plotted with the intensity converted to electron counts per second (cps) and were subjected to a multipoint baseline correction using the GRAMS AI program (version 7.01, Thermo Electron Corp., Waltham, MA). All of the measurements were conducted at room temperature (23 ± 1 °C).

Results and Discussion

Cyclic voltammograms (CVs) of a Ru-coated Au electrode obtained in deaerated 0.1 M $HClO_4$ before and after addition of methanol are shown in Figure 1. It is known that Ru dissolution occurs at potentials higher than 0.6 V,[14] which makes the comparison of CVs obtained on the same Ru electrode in solutions with and without methanol difficult. However, we found that, by cycling the Ru-coated Au electrode with a 0.1 V s^{-1} scan rate between −0.2 to +0.8 V for 10 min in 0.1 M $HClO_4$, stable CVs can be obtained. The CVs shown in Figure 1 were acquired after this treatment. Before recording CVs, the electrode was held at −0.2 V for 1 min to reduce surface oxides. The CVs were first acquired in deaerated 0.1 M $HClO_4$, and then, a measured amount of methanol was added to make up 1 M methanol in the solution. The traces obtained with (solid) and without (dotted) methanol are essentially identical (Figure 1), suggesting that methanol oxidation does not occur significantly.[14−16] The broad capacitive feature between 0.0 and 0.7 V is characteristic of RuO_2.[28,29] These observations are the same as those from the bulk Ru electrodes reported in the literature in the same potential window,[14−16] suggesting the Ru thin films used here have similar electrochemical characteristics.

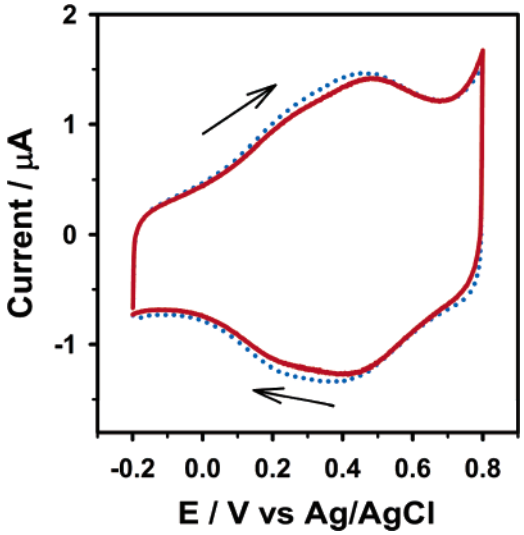

Figure 1. Cyclic voltammograms of Ru-coated Au obtained in deaerated 0.1 M $HClO_4$ with 1 M methanol (solid) and without methanol (dotted). Scan rate: 0.1 V s^{-1}. The arrows indicate the scan direction.

Potential-dependent SER spectra of Ru-coated Au acquired in 1 M methanol + 0.1 M $HClO_4$ are shown in Figure 2. The electrode was initially kept at −0.2 V in deaerated 0.1 M $HClO_4$ to reduce the Ru oxide formed during electrode transport in air from the deposition cell to the spectroelectrochemical cell. A measured amount of methanol was then added into the cell to make up a 1 M methanol solution with the potential controlled at −0.2 V. The solution was mixed and further deaerated by N_2 purging. The spectral acquisition started at −0.2 V, and the potential was stepped to more positive values in 200 mV increments after each spectrum was taken.

Below 0.2 V, the spectra are largely featureless, suggesting that the surface remains at the metallic state and methanol adsorption−oxidation does not occur in this potential region. This is different from that observed on Pt or Ru decorated Pt where methanol oxidation readily occurs and vibrational features from both M−CO and C−O stretch are observed.[1−3,21,23,30] At 0.2 V, several broad bands start to appear in the lower frequency region (Figure 2A) and these bands overlap significantly. Only the band at around 300 cm^{-1} is sharp enough that its position can be clearly identified. These features mainly arise from surface oxides,[29,31−33] indicating that surface oxidation occurs at this potential. The higher frequency region remains largely featureless. With further increase of the potential, the lower frequency bands grow and become clearer. The bands located at around 528, 640, and 710 cm^{-1} are very similar to those observed on RuO_2 thin films,[34] suggesting the formation of surface RuO_2. The 528 cm^{-1} band is the strongest among the phonon modes (lattice vibration) of the RuO_2 and serves as an indicator of the presence of the oxide.[34] The broad feature centered at around 480 cm^{-1} together with the broad features between 600 and 700 cm^{-1} has been assigned to hydrous RuO_2.[29,31−34] The assignment of the 300 cm^{-1} band is less clear. Zhang et al. tentatively assigned this to the Ru−O bending mode in their study of the oxidation of Ru-coated Au in 0.1 M $HClO_4$,[33] but it could also be from the Raman inactive lattice vibration of RuO_2, which is estimated to be at 314 cm^{-1} based on a rigid-ion model.[34] Observation of Raman inactive modes

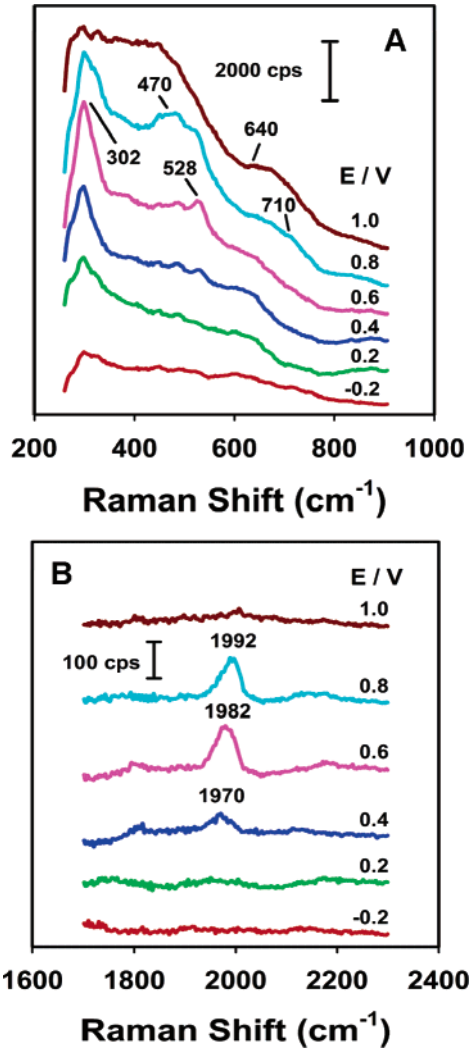

Figure 2. Potential-dependent SER spectra obtained on Ru-coated Au in 1 M methanol + 0.1 M $HClO_4$. The spectra cover both oxide vibration (A) and C−O stretch (B) frequency regions. The applied potential is indicated alongside the corresponding spectrum. The spectral acquisition started at −0.2 V toward the positive direction with 200 mV increments.

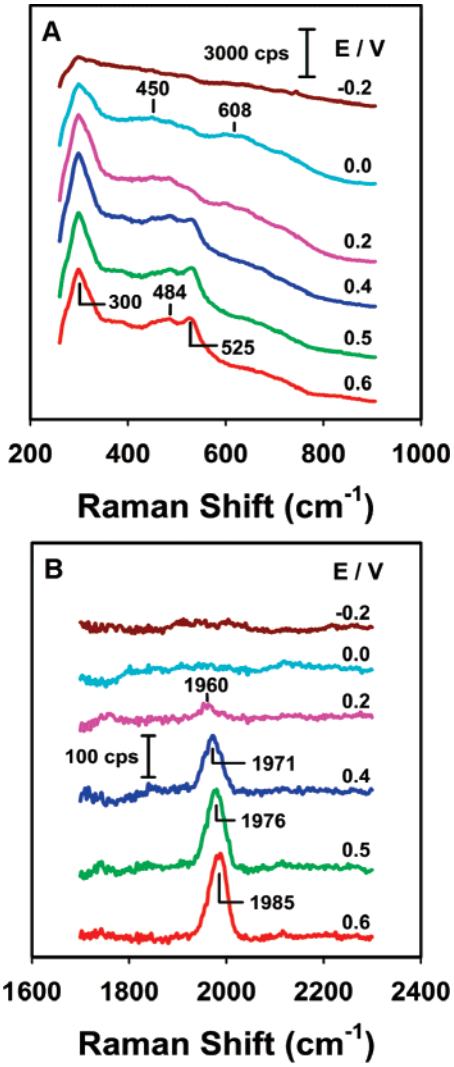

Figure 3. Potential-dependent SER spectra obtained on Ru-coated Au in 1 M methanol + 0.1 M $HClO_4$. The spectra cover both oxide vibration (A) and C−O (B) stretch frequency regions. The applied potential is indicated alongside the corresponding spectrum. The spectral acquisition started at 0.6 V toward the negative direction.

in SER spectra is well documented and is attributed to the field gradient effect and the lower symmetry of species adsorbed on the surface as compared to their free state.[35]

More interestingly, in addition to the bands from surface oxides, a new band appeared in the higher frequency region at around 0.4 V. The band intensity fully develops at 0.6 V and decreases above 0.8 V. The center frequency of this band increases from 1970 cm^{-1} at 0.4 V to 1992 cm^{-1} at 0.8 V. This band nearly completely diminishes at 1.0 V. The changes in band intensity and frequency are reversible if the potential is returned from 0.6 V, instead of increasing to 1.0 V, as shown in Figure 3. The band survives at 0.2 V but diminishes below 0 V (Figure 3B). Accompanied with these changes in the higher frequency region is the decrease of oxide band intensity (Figure 3A). We observed similar behavior on Ru in 1 M ethanol + 0.1 M $HClO_4$, but not in 1 M acetic acid + 0.1 M $HClO_4$.

Neither methanol nor perchlorate has vibration bands located in the higher frequency region. The band frequency is very similar to that observed in the electron energy loss spectra (EELS) of CO adsorbed on the RuO_2(110) surface in the ultrahigh vacuum (UHV) system,[36,37] suggesting that it is from C−O stretch of CO adsorbed on RuO_2. To confirm this band assignment, we examined SER spectra of CO adsorbed on oxidized Ru surfaces in 0.1 M $HClO_4$, as displayed in Figure 4. The surface was first fully reduced by holding the electrode at −0.2 V until the oxide bands were not discernible in the SER spectrum. Carbon monoxide was then purged into the solution for 5 min with the potential controlled at this value. The spectral acquisition started at −0.2 V toward positive direction with a 0.2 V increment till 0.8 V. The obtained spectra (not shown) agree well with those reported by Leung and Weaver.[9] The solution-phase CO was then removed by 15 min of N_2 purging while the potential was held at 0.6 V. After the solution-phase CO removal, the potential was stepped back to 0.8 V and the spectral acquisition resumed. These spectra are shown in Figure 4.

Starting with the lower frequency region (Figure 4A), several strong bands are observed. The broad envelop centered around 480 cm^{-1} is a signature of the presence of hydrous RuO_2.[29,31−34] The band at 526 cm^{-1} superimposed on the envelope, together with that at 715 cm^{-1} and the broad feature at ∼640 cm^{-1}, indicates the formation of anhydrous RuO_2.[34] The strong band at 300 cm^{-1} can be again assigned to either the Ru−O bend or the Raman inactive phonon mode of RuO_2.[33,34] The shoulder at around 460 cm^{-1} will be assigned below. The intensity of these bands decreases with the applied potential. At −0.2 V, only

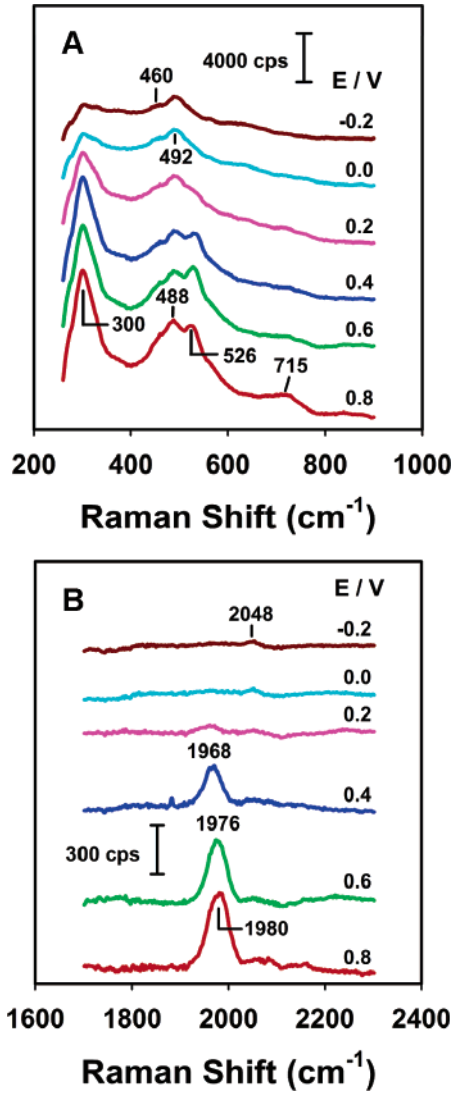

Figure 4. Potential-dependent SER spectra obtained on Ru-coated Au in 0.1 M $HClO_4$ after solution-phase CO was purged out of the solution (see text for details). The spectra cover both oxide (A) and C−O (B) vibration frequency regions. The applied potential is indicated alongside the corresponding spectrum. The spectral acquisition started at 0.8 V toward the negative direction with 200 mV decrements.

two bands located at 492 and 460 cm^{-1} are prominent. Weak vibration features from surface oxides are nonetheless discernible, indicating the surface oxide reduction is incomplete. These spectral features are similar to those observed in Figure 3.

Interestingly, at higher frequency region (Figure 4B), a band centered at 1980 cm^{-1} remains after the solution-phase CO is completely removed, indicating this band is from irreversibly adsorbed CO. In a series of EELS studies of CO adsorption and oxidation on RuO_2(110), Ertl and co-workers assigned bands at 430 (53.3 meV) and 2003 cm^{-1} (248.5 meV) to the Ru−CO (ν_{Ru-CO}) and C−O (ν_{CO}) stretches, respectively, of CO adsorbed on Ru sites with one CO interacting with a single Ru atom.[36−39] This assignment corroborates with their scanning tunneling microscopic study.[36] Compared with the EELS data, the 1980 cm^{-1} band observed here can be assigned to ν_{CO} of CO adsorbed on Ru sites. The ν_{CO} difference between the two systems probably arises from the limited spectral resolution of EELS (24 cm^{-1})[36−39] and the disparity in the oxide structure and CO coverage. The work function of RuO_2(110) is about 5.8 eV,[40] which is about 0.8 V versus the Ag/AgCl reference electrode.[41] Therefore, the lower ν_{CO} observed in the electrochemical environment is not likely from the disparity in the surface potential, which is commonly observed on metal surfaces.[41] The corresponding ν_{Ru-CO} for CO adsorbed on RuO_2 observed at 430 cm^{-1} in the UHV is very likely responsible for the shoulder at 460 cm^{-1} in the lower frequency region. This assignment agrees with the CO adsorption energy (E_{CO}) on RuO_2(110) and Ru(0001) in UHV calculated by using density functional theory (DFT).[42] On the former surface, the E_{CO} value is 1.2 eV, and on the latter, it is 1.8 eV, consistent with the measured CO desorption temperature on the two surfaces in the UHV[42] and the observed ν_{Ru-CO} at around 490 cm^{-1} on Ru in the electrochemical system.[9,30]

The intensity of the 1980 cm^{-1} band diminishes and its frequency red shifts as the potential decreases, and only a very weak feature at 2048 cm^{-1} remains at −0.2 V (Figure 4B). This potential-induced spectral transition is due to the surface reduction from RuO_2 to metallic Ru below 0.2 V and the oxidation of adsorbed CO at and above 0.2 V.[10] The weak band at 2048 cm^{-1} is from the residual CO adsorbed on the reduced Ru sites.[9,10] The ν_{CO} is higher on metallic Ru than on the RuO_2 surface, mainly because the π back-donation from the surface to the CO $2\pi^*$ orbital is stronger on the RuO_2 surface due to its higher work function.[40] At the same potential, the higher the work function, the more negatively charged the surface is and hence more back-donation. The assignment of the 2048 cm^{-1} band to ν_{C-O} on the reduced Ru agrees well with the presence of the 492 cm^{-1} band that is from the ν_{Ru-CO} of CO on metallic Ru.[9,30] The existence of the 460 cm^{-1} band suggests that the surface oxide reduction is incomplete, consistent with the observation of the weak oxide features at −0.2 V. The absence of a clear ν_{C-O} from CO adsorbed on Ru oxides is likely due to the band broadening caused by the inhomogeniety of the remaining RuO_2 domain size and the coexistence of different Ru oxidation states.[29] If the potential was stepped to 1.0 V instead of moving to the negative direction, the 1980 cm^{-1} band disappears, suggesting that the adsorbed CO can be oxidized at higher potentials. These observations closely resemble those observed above for Ru in methanol (Figures 2 and 3). The similarity between the two systems strongly suggests that the observed band in the methanol containing solution at 0.4−0.8 V is indeed from CO adsorbed on RuO_2. It should be pointed out that, in an in situ FTIR study of CO electrooxidation on the Ru(0001) surface, Lin et al. observed a ν_{CO} from 1960 to 1975 cm^{-1} at −0.2 V, when a sub-monolayer of CO_{ads} was obtained by partially oxidizing a monolayer of CO with a brief potential step to 0.45 V.[11] This is different from what we observed here where the ν_{CO} at ∼1980 cm^{-1} is only observable at potentials higher than 0.2 V.

In a recent in situ infrared reflection absorption spectroscopic study, Blizanac et al. observed a C−O stretching band centered at 1965−1994 cm^{-1} at −0.25 to 0.4 V (vs Ag/AgCl) on a reconstructed (1 × 2) Au(110) surface in 0.1 M $HClO_4$.[43] The frequency of this band is very close to the ν_{CO} seen in the present work. However, the potential-dependent behavior is very different for the two CO bands. The ν_{CO} on Au(110) is oxidized above 0.4 V and nearly absent at 0.75 V, while the CO band observed here starts to appear at 0.4 V in the methanol containing solution and reaches its maximum at 0.6−0.8 V. In addition, we have examined the SER spectra of CO adsorbed on Au electrodes without Ru; only one C−O stretching band at ∼2110 cm^{-1} was observed. These observations eliminate the possibility of assigning the 1980 cm^{-1} band to CO adsorbed on exposed Au sites that are formed above 0.6 V due to the surface oxidation and Ru oxide dissolution.

The observation of CO on RuO_2 in methanol solution suggests that methanol oxidation does occur on the polycrystalline Ru electrodes. The onset potential, 0.4 V, coincides with the potential where the methanol oxidation peak current is typically observed on Pt−Ru catalysts in cyclic voltammograms.[1−3] Methanol oxidation on the Ru(0001) surface does not occur below 0.9 V in the acidic media, as no CO was detected by in situ FTIR.[20] This disparity between polycrystalline Ru and Ru(0001) may arise from the difference in surface structure, as manifest in CO oxidation. It has been shown that CO oxidation on the Ru(0001) surface is much less facile than that on polycrystalline Ru.[44] It is therefore not surprising to observe the difference in methanol oxidation activity on these two surfaces. The fact that the ν_{CO} appears at or above 0.4 V suggests that methanol oxidation either only occurs at potentials above 0.4 V on the metallic sites or takes place on oxidized Ru sites. From the cyclic voltammograms shown in Figure 1, it is clear that methanol oxidation does not occur significantly, which corroborates with the identical chronoamperograms we obtained in 0.1 M $HClO_4$ with and without methanol by stepping the potential from −0.2 to +0.6 V. In addition, CVs acquired with a preoxidized Ru-coated Au in methanol containing solutions are identical to those obtained in the absence of methanol. This set of experiments, together with the above potential-dependent SER spectra, strongly suggests that methanol oxidation occurs at the metallic Ru sites at the potentials where surface oxidation occurs. Ru oxides are not active for methanol oxidation in the examined potential region, and therefore, their formation blocks the reaction. The more facile surface oxidation suppresses the methanol oxidation, which accounts for the absence of significant methanol oxidation current on Ru in the cyclic voltammograms obtained at room temperature. This hypothesis is further supported by the notion that no ν_{CO} was detected on the preoxidized Ru surface in the methanol solution at potentials above 0.4 V. However, if such a surface is reduced at −0.2 V and the potential is then returned to above 0.4 V, the ν_{CO} appears. It is not clear at this stage why the formed CO remains on the Ru oxide, instead of being oxidized. One plausible reason is the formation of RuO_2 is much more rapid than CO oxidation on Ru,[45] leaving CO adsorbed on the oxide. RuO_2 is not active for CO oxidation between 0.4 and 0.8 V, which is supported by its poor methanol oxidation activity.[46] The low CO oxidation activity of RuO_2 is probably due to its much higher CO diffusion barrier as compared to the metallic surfaces.[42] CO adsorbed on RuO_2(110) in the UHV has been shown to be immobile at 300 K.[42]

In summary, we demonstrate for the first time that methanol oxidation takes place on Ru surfaces at the same potential region that the reaction occurs on Pt−Ru catalysts. The observation of CO adsorbed on Ru oxide surfaces at 0.4−0.8 V suggests that Ru sites on Pt−Ru catalysts not only facilitate oxidative CO removal during methanol oxidation but also oxidize methanol themselves. The simultaneously formed surface oxide, RuO_2, however, is not active for methanol oxidation. The lack of significant methanol oxidation current in cyclic voltammograms is due to the more facile surface oxidation. Given that Ru is mostly in the metallic state in Pt−Ru catalyst, as shown by ex situ and in situ X-ray techniques,[47−49] the findings presented here suggest that at higher potentials methanol oxidation on Ru sites needs to be taken into account in the catalytic mechanism of Pt−Ru catalysts in the direct methanol fuel cell.

Acknowledgment. Acknowledgment is made to the Donors of the American Chemical Society Petroleum Research Fund for partial support of this research. We thank Professor Carol Korzeniewski of Texas Tech University for insightful discussions.

References and Notes

(1) Hamnett, A. In *Interfacial Electrochemistry. Theory, Experiment, and Applications*; Wieckowski, A., Ed.; Marcel Dekker: New York, 1999; p 843.
(2) Maillard, F.; Lu, G. Q.; Wieckowski, A.; Stimming, U. *J. Phys. Chem. B* **2005**, *109*, 16230−16243.
(3) Markovic, N. M.; Ross, P. N. *Surf. Sci. Rep.* **2002**, *45*, 121−229.
(4) Watanabe, M.; Motoos, S. *J. Electroanal. Chem.* **1975**, *60*, 267.
(5) Krausa, M.; Vielstich, W. *J. Electroanal. Chem.* **1994**, *379*, 307−314.
(6) Lin, W. F.; Zei, M. S.; Eiswirth, M.; Ertl, G.; Iwasita, T.; Vielstich, W. *J. Phys. Chem. B* **1999**, *103*, 6968−6977.
(7) Tong, Y. Y.; Kim, H. S.; Babu, P. K.; Waszczuk, P.; Wieckowski, A.; Oldfield, E. *J. Am. Chem. Soc.* **2002**, *124*, 468−473.
(8) Iwasita, T. In *Handbook of Fuel Cells—Fundamentals, Technology and Applications*; Vielstich, W., Gasteiger, H. A., Lamm, A., Eds.; John Wiley & Sons: Hoboken, NJ, 2003; Vol. 2, p 603.
(9) Leung, L. W. H.; Weaver, M. J. *Langmuir* **1988**, *4*, 1076−1083.
(10) Lin, W. F.; Iwasita, T.; Vielstich, W. *J. Phys. Chem. B* **1999**, *103*, 3250−3257.
(11) Lin, W. F.; Christensen, P. A.; Hamnett, A.; Zei, M. S.; Ertl, G. *J. Phys. Chem. B* **2000**, *104*, 6642−6652.
(12) Lin, W. F.; Christensen, P. A.; Hamnett, A. *J. Phys. Chem. B* **2000**, *104*, 12002−12011.
(13) Ikemiya, N.; Senna, T.; Ito, M. *Surf. Sci.* **2000**, *464*, L681-L685.
(14) Gasteiger, H. A.; Markovic, N.; Ross, P. N.; Cairns, E. J. *J. Phys. Chem.* **1993**, *97*, 12020−12029.
(15) Chu, D.; Gilman, S. *J. Electrochem. Soc.* **1996**, *143*, 1685−1690.
(16) Gasteiger, H. A.; Markovic, N.; Ross, P. N.; Cairns, E. J. *J. Electrochem. Soc.* **1994**, *141*, 1795−1803.
(17) Kardash, D.; Korzeniewski, C.; Markovic, N. *J. Electroanal. Chem.* **2001**, *500*, 518−523.
(18) Lin, W. F.; Christensen, P. A. *Faraday Discuss.* **2002**, *121*, 267−284.
(19) Lin, W. F.; Christensen, P. A.; Hamnett, A. *Phys. Chem. Chem. Phys.* **2001**, *3*, 3312−3319.
(20) Lin, W. F.; Jin, J. M.; Christensen, P. A.; Scott, K. *Electrochim. Acta* **2003**, *48*, 3815−3822.
(21) Tian, Z. Q.; Ren, B. *Annu. Rev. Phys. Chem.* **2004**, *55*, 197.
(22) Weaver, M. J.; Zou, S. Z.; Chan, H. Y. H. *Anal. Chem.* **2000**, *72*, 38A−47A.
(23) She, C. X.; Xiang, J.; Ren, B.; Zhong, Q. L.; Wang, X. C.; Tian, Z. Q. *J. Korean Electrochem. Soc.* **2002**, *5*, 221.
(24) Gao, P.; Gosztola, D.; Leung, L. W. H.; Weaver, M. J. *J. Electroanal. Chem.* **1987**, *233*, 211.
(25) Strbac, S.; Maroun, F.; Magnussen, O. M.; Behm, R. J. *J. Electroanal. Chem.* **2001**, *500*, 479−490.
(26) Gruenbaum, S. M.; Henney, M. H.; Kumar, S.; Zou, S. Z. *J. Phys. Chem. B* **2006**, *110*, 4782−4792.
(27) Jaiswal, A.; Tavakoli, K. G.; Zou, S. Z. *Anal. Chem.* **2006**, *78*, 120−124.
(28) Burke, L. D.; Murphy, O. J. *J. Electroanal. Chem.* **1979**, *101*, 351.
(29) Mo, Y. B.; Cai, W. B.; Dong, J. A.; Carey, P. R.; Scherson, D. A. *Electrochem. Solid State Lett.* **2001**, *4*, E37−E38.
(30) Yang, H.; Yang, Y.; Zou, S. Z. Manuscript in preparation.
(31) Chan, H. Y. H.; Takoudis, C. C.; Weaver, M. J. *J. Catal.* **1997**, *172*, 336−345.
(32) Chan, H. Y. H.; Zou, S. Z.; Weaver, M. J. *J. Phys. Chem. B* **1999**, *103*, 11141−11151.
(33) Zhang, Y.; Gao, X. P.; Weaver, M. J. *J. Phys. Chem.* **1993**, *97*, 8656−8663.
(34) Bhaskar, S.; Dobal, P. S.; Majumder, S. B.; Katiyar, R. S. *J. Appl. Phys.* **2001**, *89*, 2987−2992.
(35) Moskovits, M. *Rev. Mod. Phys.* **1985**, *57*, 783.
(36) Kim, S. H.; Paulus, U. A.; Wang, Y.; Wintterlin, J.; Jacobi, K.; Ertl, G. *J. Chem. Phys.* **2003**, *119*, 9729−9736.
(37) Paulus, U. A.; Wang, Y.; Jacobi, K.; Ertl, G. *Surf. Sci.* **2003**, *547*, 349−354.
(38) Fan, C. Y.; Wang, J.; Jacobi, K.; Ertl, G. *J. Chem. Phys.* **2001**, *114*, 10058−10062.
(39) Wang, J.; Fan, C. Y.; Jacobi, K.; Ertl, G. *Surf. Sci.* **2001**, *481*, 113−118.
(40) Kim, Y. D.; Seitsonen, A. P.; Wendt, S.; Wang, J.; Fan, C.; Jacobi, K.; Over, H.; Ertl, G. *J. Phys. Chem. B* **2001**, *105*, 3752−3758.
(41) Weaver, M. J.; Zou, S. Z.; Tang, C. *J. Chem. Phys.* **1999**, *111*, 368−381.

(42) Over, H.; Kim, Y. D.; Seitsonen, A. P.; Wendt, S.; Lundgren, E.; Schmid, M.; Varga, P.; Morgante, A.; Ertl, G. *Science* **2000**, *287*, 1474−1476.

(43) Blizanac, B. B.; Arenz, M.; Ross, P. N.; Markovic, N. M. *J. Am. Chem. Soc.* **2004**, *126*, 10130−10141.

(44) Marinkovic, N. S.; Wang, J. X.; Zajonz, H.; Adzic, R. R. *Electrochem. Solid State Lett.* **2000**, *3*, 508−510.

(45) Gasteiger, H. A.; Markovic, N.; Ross, P. N.; Cairns, E. J. *J. Phys. Chem.* **1994**, *98*, 617−625.

(46) Kennedy, B. J.; Smith, A. W. *J. Electroanal. Chem.* **1990**, *293*, 103−110.

(47) Viswanathan, R.; Hou, G. Y.; Liu, R. X.; Bare, S. R.; Modica, F.; Mickelson, G.; Segre, C. U.; Leyarovska, N.; Smotkin, E. S. *J. Phys. Chem. B* **2002**, *106*, 3458−3465.

(48) O'Grady, W. E.; Hagans, P. L.; Pandya, K. I.; Maricle, D. L. *Langmuir* **2001**, *17*, 3047−3050.

(49) Kim, H.; de Moraes, I. R.; Tremiliosi, G.; Haasch, R.; Wieckowski, A. *Surf. Sci.* **2001**, *474*, L203−L212.